Macromolecules
ARTICLE

Macromolecules **2010**, *43*, 4161–4171 **4161**
DOI: 10.1021/ma100299p

Crystal Structure and Morphology of Linear Aliphatic *n*-Polyurethanes

C. E. Fernández,[†] M. Bermúdez,[†] S. Muñoz-Guerra,*[,†] S. León,[‡] R. M. Versteegen,[§] and E. W. Meijer[§]

[†]*Departament d'Enginyeria Química, Universitat Politècnica de Catalunya, ETSEIB, Diagonal 647, Barcelona 08028, Spain,* [‡]*Departamento de Ingeniería Química, Universidad Politécnica de Madrid, ETSII, Gutiérrez Abascal 2, Madrid 28006, Spain, and* [§]*Laboratory of Macromolecular and Organic Chemistry, Eindhoven University of Technology, P.O. Box 513, NL-5600 MB Eindhoven, The Netherlands*

Received February 9, 2010; Revised Manuscript Received March 24, 2010

ABSTRACT: The crystal structure and morphology of a series of linear aliphatic polyurethanes with generic formula $-(CH_2)_nOCONH-$ and containing from 5 to 12 methylene units have been investigated by using TEM combined with X-ray and electron diffraction analysis. Lamellar crystals with a thickness ranging between 5 and 10 nm displaying a variety of crystal habits were obtained by isothermal crystallization from diluted solution in different solvents. A crystal structure similar to that described for the layered α-form of nylons seems to be commonly adopted by these polyurethanes. It essentially consists of a triclinic lattice made of hydrogen-bonded sheets with chains in fully extended conformation. Chains within the sheets are arranged in the *antiparallel* mode giving a normal scheme of hydrogen bonds. Sheets are stacked along the *b*-axis and progressively shifted along both *a* and *c* axes. The interchain and intersheet distances in this lattice are of values similar to those found in nylons. Energy calculations were in agreement with the arrangement proposed for chain packing. X-ray diffraction recorded from heated samples at real times showed that none of these polyurethanes undergoes Brill transition although odd members displayed structural changes concomitant with the occurrence of an unfinished ongoing process. The IR analysis at variable temperature revealed that approximately 50% of hydrogen bonds were retained upon heating at temperatures fairly above melting.

Introduction

Linear polyurethanes are a well-known class of polymers of great industrial significance and with a broad range of applications.[1,2] They may be aliphatic or aromatic, and depending on whether one difunctional monomer or two complementary bifunctional monomers are used for polymerization, they are classified as A·B or AA·BB types, respectively. Aliphatic AA·BB-type polyurethanes, abbreviated as *m,n*-PUR, are nondirectional polymers usually obtained by step-growth polyaddition of α,ω-alkanediols to diisocyanates containing *m* and *n* carbon atoms, respectively.[3] Aliphatic A·B-type polyurethanes, abbreviated as *n*-PUR, consist of directional chains made from α,ω-isocyanate alcohols containing *n* carbon atoms. Whereas *m,n*-PUR are easily attainable and widely spread materials, *n*-PUR are relatively uncommon due to the difficult access to the monomers required for their synthesis. Nevertheless, we have described a reliable method of preparation of *n*-PUR from α,ω-amino alcohols that makes these polymers much more available.[4] Later other useful methods of preparation for *n*-PUR from amino alcohols have been published.[5,6]

From the point of view of their chemical constitution, polyurethanes may be envisaged to be hybrid between polyamides and polyesters inasmuch the urethane group includes both the amide and the ester groups. Even so, the overall pattern of behavior of polyurethanes is closer to polyamides because their ability to form hydrogen bonds using the "amide" moiety of the urethane group. In fact, linear aliphatic polyurethanes may be considered as deriving from nylons with the same number of atoms in the main chain, in which the α-methylene unit has been replaced by an oxygen atom (Scheme 1). Most of the linear polyurethanes are semicrystalline polymers displaying large crystallinity and fairly high melting temperatures,[3] and the structure of aliphatic *m,n*-PUR has been largely investigated in the past. Kinoshita et al.[7,8] described the crystal structure of these polyurethanes as being very similar to that found in nylons of AA·BB-type and later work made on very long chain members has confirmed the close structural resemblance existing between these two polymer families.[9−11] In all reported cases, polyurethanes adopt the typical structure of polyamides with chains in fully extended conformation and packed in a crystal lattice made of hydrogen-bonded sheets. On the contrary, the information on hand about the structure of *n*-PUR is actually meager. Leaving aside some characterization data published as complementary to synthetic work,[4,5] it is restricted to a couple of recently published articles dealing with their thermal properties and crystallization behavior.[12,13] To the best of our knowledge, the crystalline structure of *n*-PUR has not been investigated to date in any aspect.

In this paper, we wish to report on the crystal structure and morphology of the *n*-PUR family for *n* values from 5 to 12. Diffraction data provided by X-ray and electron diffraction of both pristine powder and lamellar crystals grown in solution are analyzed and interpreted with the support of energy calculations. Since *n*-PUR are structurally analogous to *n*-nylons, the elucidation of the structure has been made by relying largely on the wide knowledge that has been coined on these polyamides.[14] Depending on the nylon and crystallization conditions, two crystal forms, named α and γ forms, are known to be adopted by *n*-nylons. The α-form, described for the first time by Holmes et al.[15] consists of a layered array of hydrogen-bonded sheets with chains in fully extended conformation and stacked with a separating spacing around 0.37 nm. The γ-form is a hexagonal or *quasi*-hexagonal array of 2-fold helices separated 0.41 nm with

*Corresponding author: sebastian.munoz@upc.edu.

Published on Web 04/12/2010

hydrogen bonds running along a unique direction within the crystal.[16] Several modifications may exist for the α-form which vary in the pattern in which neighboring chains are arranged in the crystal lattice.[17,18] Whereas odd-nylon chains within the hydrogen-bonded sheets may be arranged in either *parallel* or *antiparallel* mode, i.e., following an oblique or normal scheme of hydrogen bonds, respectively, only the later is feasible for even-nylons provided that all hydrogen bonds are comfortably made. Furthermore, hydrogen-bonded sheets made of odd-nylons are polar whereas those made of even nylons are nonpolar since the CO dipoles become canceled out in this case due to the two opposite orientations adopted by the amide groups.[19,20]

With the purpose of making comparison of *n*-PUR with nylons more straightforward, in this study the value of *n* has been made to correspond to the number of carbons contained in the uninterrupted polymethylene segment. In this way, *n*-PUR compare perfectly to (*n* + 2) nylons since they have the same even−odd parity, contain the same number of backbone atoms in the repeating unit and share the same scheme of hydrogen bonds (Scheme 2).

Scheme 1. Compared Chemical Structures of Nylons and Polyurethanes

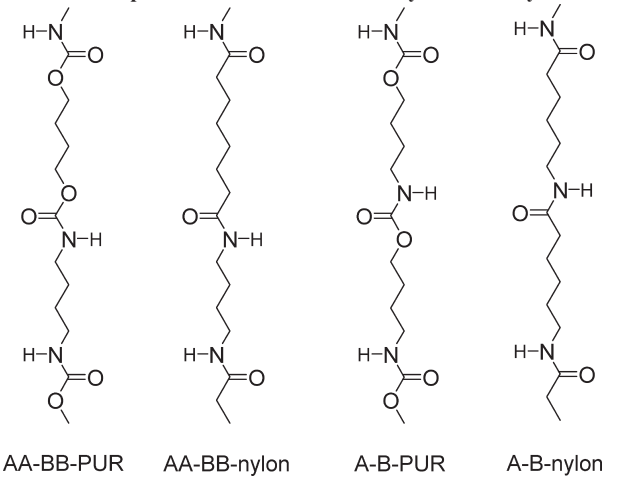

Experimental Section

Materials. The polyurethanes used in this study were obtained by polyaddition of the corresponding α,ω-isocyanate alcohols, which were synthesized by reaction of α,ω-amino alcohols with di-*tert*-butyl tricarbonate. A detailed account of the synthesis and chemical characterization of these polyurethanes has been reported elsewhere.[4] Some data of *n*-PUR of outstanding relevance in the context of this work are given in Table 1.

Methods. Crystallization of *n*-PUR was accomplished isothermally from diluted polymer solutions (0.1% w/w). A variety of solvents like glycerin, triethylene glycol (TEG), propylene carbonate (PC), and several alkanols, were used at different crystallization temperatures. Crystal growing was monitored by phase-contrast optical microscopy and the grown crystals were

Table 1. Molecular Weights and Thermal Data of *n*-PUR.[a]

n-PUR	L^b (nm)	$M_w{}^c$	PD^c	$T_m{}^d$ (°C)	$\Delta H_m{}^d$ (J·g^{-1})	$T_g{}^e$ (°C)	${}^0T_m{}^f$ (°C)
5-PUR	0.98	22 300	1.5	127	90	13.5	171
6-PUR	1.10	34 400	1.4	157	112	10.5	191
7-PUR	1.22	26 500	1.5	114	63	2.5	131
8-PUR	1.35	30 500	1.6	146	120	−1.0	185
9-PUR	1.46	67 400	1.6	116	116	−1.0	136
10-PUR	1.59	32 600	1.7	148	127	−6.0	162
11-PUR	1.71	20 300	1.5	119	115	n.o	138
12-PUR	1.84	21 400	1.6	141	128	n.o	157

[a] Experimental data taken from refs 4 and 13. [b] Length of the CRU in fully extended conformation $L_0 = l(n + 3)$ taking 0.122 nm as the average length bond. [c] Weight-average molecular weight and polydispersity degree determined by GPC. [d] Melting temperature and enthalpy determined by DSC at a heating rate of 10 °C·min^{-1} from synthesis samples. [e] Glass transition determined by DSC at a heating rate of 20 °C·min^{-1} from quenched samples. [f] Equilibrium melting temperature determined according to Hoffman and Weeks.

Scheme 2. Possible Chain Arrangements in Hydrogen-Bonded Sheets Made of Odd and Even *n*-PUR

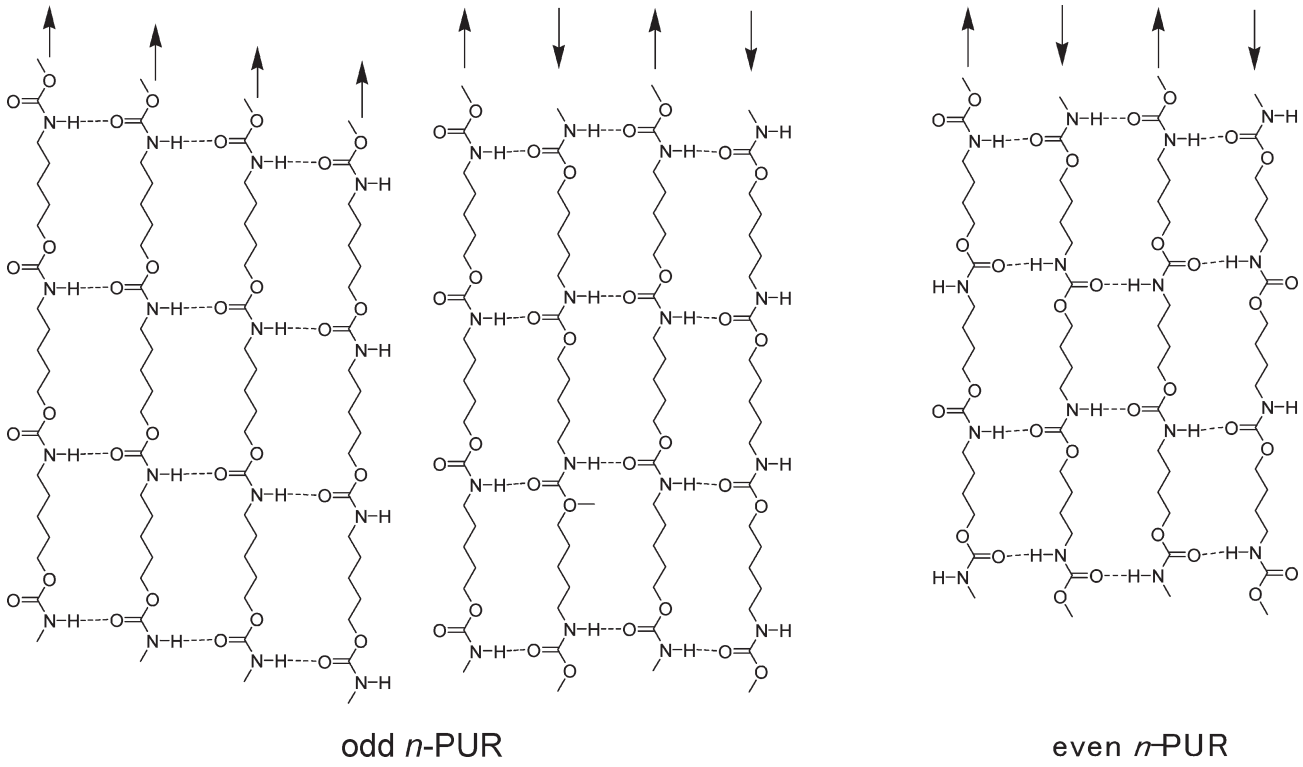

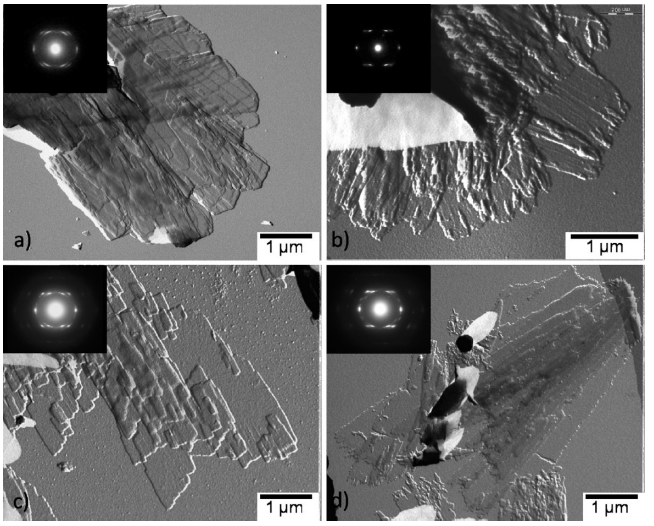

Figure 1. TEM micrographs of lamellar crystals of odd *n*-PUR crystallized at 90 °C in the indicated solvents. Key: (a) 5-PUR in glycerin, (b) 7-PUR in TEG, (c) 9-PUR in TEG, and (d) 11-PUR in TEG. Insets: ED patterns of the corresponding lamellae.

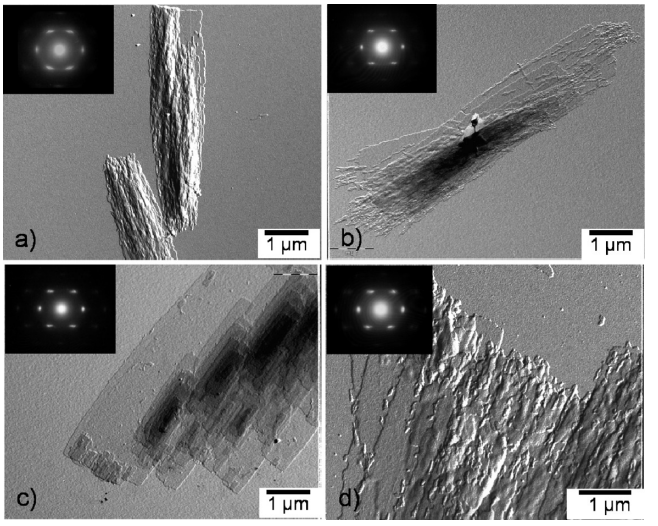

Figure 2. TEM micrographs of lamellar crystals of even *n*-PUR crystallized in PC at the indicated temperatures. Key: (a) 6-PUR at 117 °C, (b) 8-PUR at 115 °C, (c) 10-PUR at 110 °C, and (d) 12-PUR at 105 °C. Insets: ED patterns of the corresponding lamellae.

recovered by centrifugation, repeatedly washed with 1-butanol and stored in suspension in this solvent until used. Crystal mats to be examined by X-ray diffraction were prepared by slow filtering of the 1-butanol crystal suspensions. A total of 20−30 mg of polymer was crystallized in order to obtain the minimum amount of sediment required for this analysis.

X-ray diffractograms from powders were obtained in a Debye−Scherrer camera INEL CPS-120 provided with a detector sensible to position 120° and 4096 measuring channels, and using acquisition times of 3600 s. X-ray diffraction patterns from crystal mats were recorded on photographic films using a modified Statton camera and calibrated with molybdenum sulfide powder (d_{002} = 0.6147 nm). CuK_α radiation of wavelength 0.1541 nm was used in all these diffraction experiments. X-ray diffraction data from heated samples were taken at real time using synchrotron light in the B16 line of ERSF (Grenoble, France) or A2 line of DEYSY (Hamburg, Germany). Transmission electron microscopy (TEM) observations were carried out on a Philips-Tecnai instrument operating at 80 and 100 kv for bright field (digital camera attached) and electron diffraction (photographic film), respectively. Electron diffraction (ED) was recorded in the selected area mode and patterns were internally calibrated with gold (d_{111} = 0.235 nm). Samples for observation were prepared by depositing a drop of the 1-butanol crystal suspension on freshly prepared carbon coated grids. Crystals to be observed in the bright field mode were shadowed with platinum−carbon at an angle of approximately 15° whereas unshadowed samples were used for electron diffraction analysis. Infrared spectra were acquired on a Perkin-Elmer FTIR 2000 spectrometer with a resolution of 4 cm^{-1}. Spectra from heated samples were obtained using a variable temperature cell P/N 21525 with a precision of ±5 °C.

Results and Discussion

Lamellar Crystals of *n*-PUR. The crystallization of *n*-PUR from diluted solution was carried out in a variety of solvents with the purpose of obtaining lamellar crystals with morphologies and sizes suitable for electron diffraction analysis. Results were largely dependent on the even−odd parity of the polyurethane, the selection of appropriate solvents being much more restrictive for odd than for even *n*-PUR. A representative assortment of lamellar crystals of odd *n*-PUR crystallized at 90 °C in either glycerin or TEG is shown in Figure 1. Attempts made to obtain lamellae of 7-, 9-, and 11-PUR in glycerin afforded poorer results than when TEG was used whereas 5-PUR could not be crystallized in TEG. Furthermore, the crystal morphology displayed by *n*-PUR was found to be extremely sensitive to crystallization conditions to the point that quite dissimilar morphologies were obtained in different experiments made under the same conditions (some additional pictures of odd *n*-PUR crystallized in TEG are provided in the ESM file for illustration). Nevertheless, multilamellar elongated crystals with a more or less rectangular shape and several micrometers width were obtained in all cases. Since crystals did not grow as isolate entities, they became unavoidably piled up upon deposition on the carbon film making their detailed morphological analysis difficult. Surface striations and serrated edges, which are described in the literature as typical features of nylon lamellae,[21,22] and in particular of odd nylon lamellae,[19] are displayed in most of cases. The thickness of the individual lamellae estimated from their shadow lengths oscillates between 4 and 8 nm, the value increasing progressively with the value of *n*.

Crystallization of even *n*-PUR in both PC and TEG solvents afforded really good results. Selected pictures of lamellar crystals grown in these two solvents are shown in Figures 2 and 3, respectively. It is seen that more or less isolated multilayered platelets displaying features similar to those typical of nylon lamellae were obtained in all cases. As before, the rectangular or oblique shape appears to be the usual habit displayed by even *n*-PUR lamellae, and it is also worthy to note the presence of corrugations at the crystal surfaces and serrated front growing edges in most of them. Particularly large sizes were obtained in TEG with lamellar widths attaining up to several tenths of micrometers. The lamellar height was confined again within the 4−9 nm range and shows the same trend with *n* as indicated before for the odd series. Even *n*-PUR could be also successfully crystallized from aliphatic alcohols rendering lamellar crystals much more elongated than in the other solvents but having similar thickness. Illustrative pictures of these needle-like lamellar crystals are provided in the ESM file.

Essentially the same selected area ED pattern was produced by all *n*-PUR lamellar crystals regardless the length or parity of the polymethylene segment, or even the temperature or solvent used for crystallization. Notwithstanding,

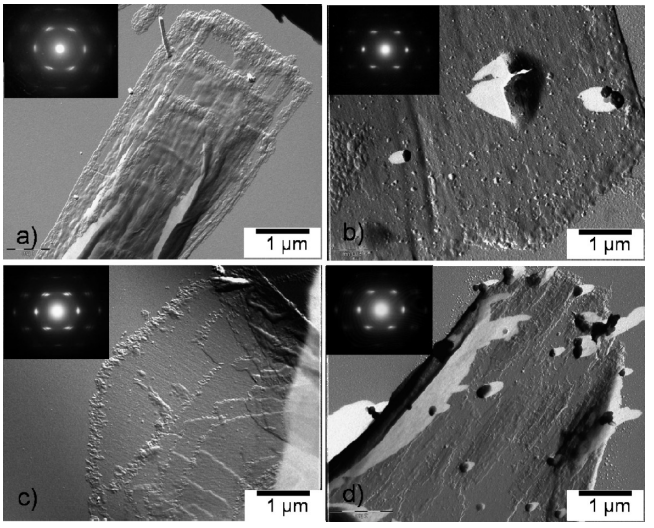

Figure 3. TEM micrographs of lamellar crystals of even *n*-PUR crystallized in TEG at the indicated temperatures. Key: (a) 6-PUR at 120 °C, (b) 8-PUR at 120 °C, (c) 10-PUR at 135 °C, and (d) 12-PUR at 105 °C. Insets: ED patterns of the corresponding lamellae.

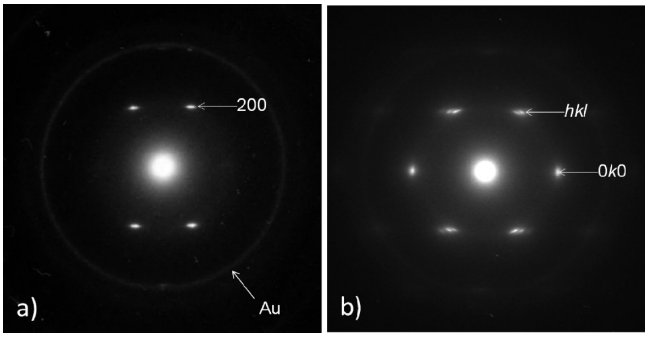

Figure 4. ED pattern of 10-PUR single crystal. (a) Untilted. (b) Tilted ~30° around the long dimension of the lamella.

ED patterns were found to be extremely sensitive to crystal tilting as it is illustrated in Figure 4 for the particular case of 10-PUR. The pattern registered from untilted crystals consisted of two symmetrical pairs of sharp reflections with a spacing of 0.44−0.43 nm and oriented at an angle close to 30° respect to the long dimension of the crystal. Upon tilting of the specimen under observation at an angle around 30°, the pattern retained the *mm* symmetry but the single reflections were replaced by a row of closely spaced spots covering a range of spacings of 0.45−0.35 nm. Simultaneously, a new pair of strong reflections with a spacing of 0.38−0.37 nm and oriented normally to the long crystal side came into view. According to nylon antecedents, hydrogen-bonded sheets in these crystals should be expected to be aligned with hydrogen bonds pointing to the fastest growing front of the crystal. The changes observed upon tilting are therefore a clear indication that sheets must be tilted with respect to the lamellar surface normal in a similar way as it uses to happen nylons crystallized in the α-form.[23] The symmetry displayed by the pattern is attributed to the occurrence of twinning, which is also a frequent phenomenon taking place in nylons.[21,22,24] Accordingly, *n*-PUR lamellar crystals are interpreted to consist of twinned domains with the hydrogen-bonded sheet plane being the only composition plane. A scheme of the ED pattern is depicted in Figure 5 together with a draft of the projected crystal lattice from which it arises. Interpretation of the ED pattern was made on the

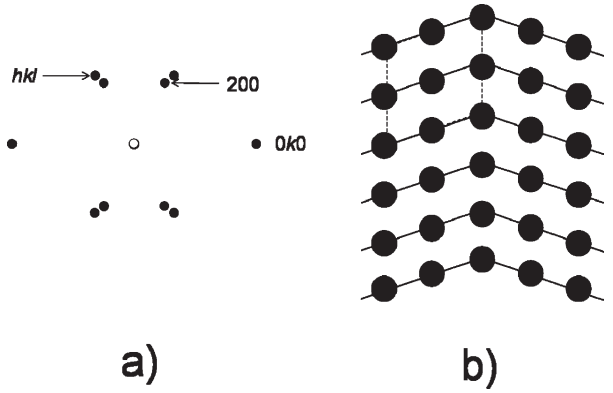

Figure 5. Scheme of the electron diffraction pattern recorded from lamellar crystals of *n*-PUR (a) and the lattice from which it arises (b).

following premises: (a) The 0.38−0.37 nm reflection is associated with the distance between adjacent hydrogen-bonded sheets and therefore indexed as 0*k*0 (*k* = 1 or 2). (b) Hydrogen bonds run along the *a*-axis with a distance between hydrogen-bonded chains of 0.48−0.49 nm; hydrogen-bonded chains are assumed to be in *antiparallel* arrangement (normal scheme) so that the *a* parameter of the unit cell needs to be doubled to accommodate two chains in opposite orientation. (c) Because of the fact that chains are leaning in the lamella, all the *hk*0 planes other than *h*00 planes fall out the Ewald sphere and they become therefore missing in the untilted ED pattern; as expected, they come into view when the sample is tilted in the microscope at angles close to the chain tilting angle.

The ED pattern obtained for each *n*-PUR is shown in the inset attached to its respective bright field image in Figures 1, 2, and 3. All spacings values measured by electron diffraction of lamellar crystals together with those provided by X-ray diffraction (see below) for the whole family of *n*-PUR studied in this work are listed in Tables 2 and 3.

Powder X-ray Diffraction of *n*-PUR. The X-ray diffraction profiles recorded in the medium to wide-angle range from powdered samples of *n*-PUR coming directly from synthesis are shown in Figure 6 where even and odd members are separately compared. Two intense peaks at *d*-spacings of ~0.44 nm and ~0.38 nm are seen in the wide-angle region of odd *n*-PUR (Figure 6a). The profiles obtained for even *n*-PUR also display these two diffraction peaks although at slightly lower spacings (0.43 and 0.37 nm), and accompanied by a third peak at a *d*-spacing of 0.40−0.41 nm. This latter peak gradually decays in intensity with increasing value of *n* to become almost absent in the profile of 12-PUR (Figure 6b). In addition to the main peaks, a weak or very weak peak below $2\theta \sim 15°$ is also detected for both series, even and odd. The exact position of this peak steadily shifts to smaller angles with increasing values of *n*. According to the information provided by ED, it becomes clear that spacings observed in the wider angle region must be related to the side-by-side packing of the chains whereas those appearing at smaller angles should arise from 00*l* planes.

Attempts to obtain oriented samples from *n*-PUR by pulling and stretching fibers proved unsuccessful, in part because severe limitations in the amounts of available material existed. On the other side, mats exhibiting partial orientation could be prepared by quiet filtration of 1-butanol suspensions of *n*-PUR lamellar crystals. The X-ray diffraction patterns obtained from edge-viewed 6-, 11-, and 12-PUR mats are shown in Figure 7. Three arced reflections are seen in the wide angle region of the pattern coming from

Table 2. Diffraction Data and Crystal Parameters of Odd *n*-PUR

d (obsd)[a]								
powder	lamellar crystals						density[e] (g·mL^{-1})	
WAXS	ED	WAXS	*hkl*[b]	*d* (calcd)[b]	unit cell[c] (nm, deg)	N^d	measd	calcd
				5-PUR				
0.605 m		0.605 m	001	0.598	$a = 0.98$; $b = 1.28$; $c = 0.98$	4	1.20	1.19
0.435 s	0.435 s	0.440 s	200	0.444	$\alpha = 40.4°$; $\beta = 90°$; $\gamma = 74.1°$			
0.370 s	0.375 s	0.370 s	020, 220	0.376, 0.376				
	0.240 w		420	0.235				
				7-PUR				
0.820 w			001	0.820	$a = 0.98$; $b = 1.18$; $c = 1.22$	4	1.15	1.15
0.450 s	0.445 s	0.450 s	200	0.446	$\alpha = 45.0°$; $\beta = 90°$; $\gamma = 72.9°$			
0.390 s		0.380 s	020 220	0.379, 0.376				
				9-PUR				
0.980 m		0.98 m	001	0.981	$a = 0.98$; $b = 1.18$; $c = 1.46$	4	1.14	1.13
0.450 s	0.445 s	0.450 s	200	0.446	$\alpha = 44.9°$; $\beta = 90°$; $\gamma = 73°$			
0.375 s		0.385 s	020 220	0.379,0.376				
				11-PUR				
1.190 m		1.190 m	001	1.189	$a = 0.98$; $b = 1.15$; $c = 1.71$	4	1.10	1.11
0.450 s	0.445 s	0.450 s	200	0.445	$\alpha = 46.8°$; $\beta = 90°$; $\gamma = 72.3°$			
0.390 s		0.380 s	020, 220	0.381, 0.377				

[a] Bragg spacing (in nm) experimentally determined by X-ray and electron diffraction with indication of visually estimated intensity (s: strong, m: medium, w: weak). [b] Indexing and spacings (in nm) calculated on the basis of their respective unit cells. [c] Unit cell parameters determined on the basis of observed diffraction data. [d] Number of CRU (chemical repeating unit) contained in the unit cell. [e] Density measured in MeOH−glycerin mixtures by the flotation method and calculated for the proposed unit cell.

Table 3. Diffraction Data and Crystal Parameters of Even *n*-PUR

d (observed)[a]								
powder	lamellar crystals						density[e] (g·mL^{-1})	
WAXS	ED	WAXS	*hkl*[b]	*d* (calcd)[b]	unit cell[c] (nm, deg)	N^d	measd	calcd
				6-PUR				
0.760 w		0.760 s	002	0.766	$a = 0.96$; $b = 0.55$; $c = 2.20$	4	1.17	1.22
0.430 s	0.430 s	0.430 s	200	0.437	$\alpha = 46.8°$; $\beta = 90°$; $\gamma = 72.5°$			
0.400 s	0.400 s	0.400 s	201, 211	0.391, 0.399				
0.365 s	0.365 s	0.365 vw	010, 210	0.366, 0.365				
0.240 w	0.240 w	0.235 w	410	0.240				
				8-PUR				
0.970 w		0.970 w	002	0.972	$a = 0.96$; $b = 0.55$; $c = 2.70$	4	1.10	1.17
0.430s	0.430 s	0.440 s	200	0.430	$\alpha = 49.2°$; $\beta = 90°$; $\gamma = 70.3°$			
0.400 m		0.410 s	201, 211	0.395, 0.404				
0.370 s		0.380 s	010, 210	0.373, 0.377				
0.240 w		0.240 vw	410	0.237				
				10-PUR				
1.135 w		1.120 w	002	1.137	$a = 0.96$; $b = 0.55$; $c = 3.19$	4	1.09	1.17
0.430 s	0.430 s	0.440 s	200	0.430	$\alpha = 48.6°$; $\beta = 90°$; $\gamma = 70.5°$			
0.410 w		0.400 s	201, 211	0.400, 0.398				
0.370 s		0.375 s	010, 210	0.369, 0.374				
				12-PUR				
1.280 m		1.280 m	002	1.281	$a = 0.96$; $b = 0.56$; $c = 3.68$	4	1.08	1.16
0.430 s	0.430 s	0.430 s	200	0.430	$\alpha = 47.3°$; $\beta = 90°$; $\gamma = 70.9°$			
0.370 s		0.370 s	010, 210	0.368, 0.374				

[a] Bragg spacing (in nm) experimentally determined by X-ray and electron diffraction with indication of visually estimated intensity (s: strong, m: medium, w: weak). [b] Indexing and spacings (in nm) calculated on the basis of their respective unit cells. [c] Unit cell parameters determined on the basis of observed diffraction data. [d] Number of CRU (chemical repeating unit) contained in the unit cell. [e] Density measured in MeOH−glycerin mixtures by the flotation method and calculated for the proposed unit cell.

6-PUR. The innermost reflection (0.42−0.43 nm) is equatorially oriented whereas the outermost one (0.37−0.38 nm) is off-meridional. The intermediately located reflection with spacing at ∼0.41 nm displays an intermediate orientation. In agreement with diffraction results obtained from powdered samples (see above and Figure 6) this reflection does not appear in 12-PUR and it is also absent in all odd *n*-PUR. On the other hand, the scattering observed in the

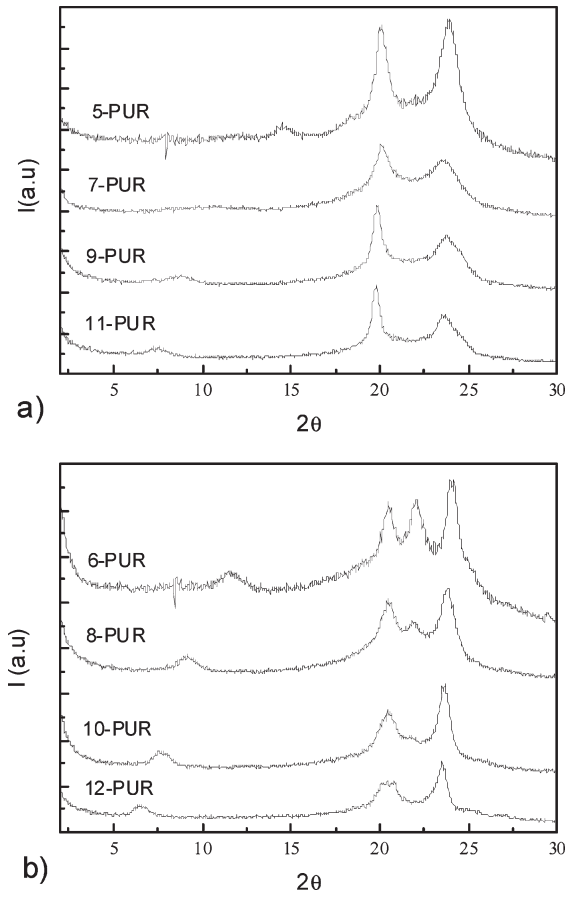

Figure 6. WAXS profiles of *n*-PUR registered from synthesis powder: (a) odd *n*-PUR and (b) even *n*-PUR.

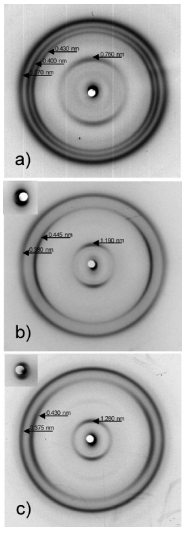

Figure 7. WAXS patterns of lamellar crystal mats: (a) 6-PUR, (b)11-PUR, and (c) 12-PUR. Insets in parts b and c: Low angle reflections associated with the lamellar thickness.

medium-low angle region is meridionally oriented and it must be therefore related to the basal planes of the crystal lattice or even to higher orders of the scattering of the lamella itself. The spacing appearing in this group between 0.6 and 1.2 nm (which is indexed as 001 or 002 for odd and even *n*-PUR, respectively) along with the length of the chemical repeating unit (CRU) of each *n*-PUR in fully extended planar conformation, L_0, are plotted against *n* in Figure 8. The 00*l*

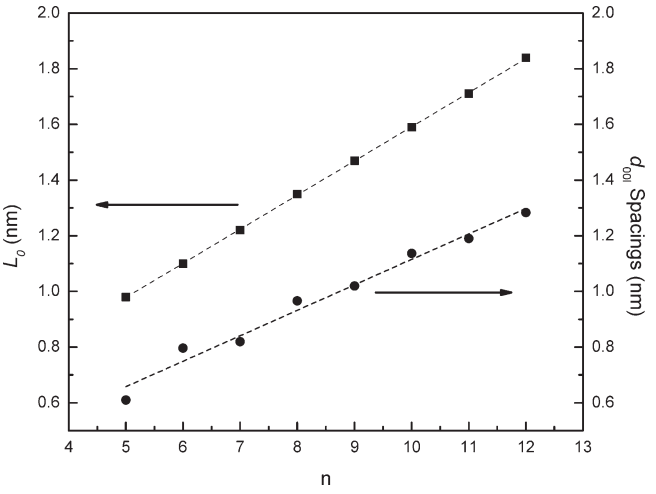

Figure 8. Length of the fully extended CRU (L_0) and 00*l* spacing of *n*-PUR *vs n* (*l* = 1 or 2 for odd or even values of *n*, respectively).

spacing is seen to increase almost linearly with *n* and to correlate well with the CRU length value.

The diffraction analysis of these lamellar mats, in spite of their moderate orientation, was proven to be extremely helpful for the elucidation of the crystalline structure of *n*-PUR given the inaccessibility to fiber samples. The information provided by the mat patterns strongly supported the interpretation made of the lamellar ED patterns regarding side-by-side chain packing. Furthermore, it corroborated that lamellae must be horizontally deposited with chains tilted to the mat axis affording substantial evidence on the orientation of *hk*0 planes within the lamella. On the basis of this information, the medium-angle reflections could be indexed without ambiguity as 00*l*.

Crystal Structure of *n*-PUR. The information provided by ED and WAXS analysis allowed putting forward a crystal structure for *n*-PUR at the medium level of accuracy. In order to fit the two *hk*0 spacings observed by X-ray diffraction, the projected unit cell parameters were determined for all the members of the series on the condition that $d_{200} \approx 0.44$ nm and $d_{220} \approx d_{020} \approx 0.38$ nm. A detailed account of calculations leading to the determination of unit cell parameters is given in the ESM file. Hydrogen bonds within the sheets set between *antiparallel* chains following the normal scheme and making $\beta = 90°$. A value of *a* between 0.960 and 0.980 nm corresponding to the double of the interchain distance was assumed according to most of antecedents on hydrogen-bonded structures in nylons.[15,23] The unit cell was established by taking *c* equal to L_0 (the extended *n*-PUR constitutional repeating unit). A triclinic unit cell with $a =$ 0.980 nm, $c = (n + 3) \times 0.122$ nm and $\beta = 90°$, and α and γ angles slightly oscillating around 45° and 73° depending on the *n* value was able to explain all the diffraction data gathered for the whole series of odd *n*-PUR. In this structure hydrogen-bonded sheets are stacked along the *b*-axis and sheared by a constant displacement of 0.35−0.40 nm along both *a*-axis and *c*-axis. As the sheets are polar (all C═O bonds within the sheet are pointing to the same direction) two arrangements are feasible for adjacent sheets leading to a polar or nonpolar lattice, respectively. As it is mostly described for odd nylons, a structure with neighboring sheets in alternating orientation so that amide dipoles become canceled out, is assumed to occur in odd *n*-PUR. It is noteworthy that the shift of the sheets along the *c*-axis corresponds roughly to the displacement of one −O−C−N− main chain sequence so that the urethane groups become homogenously

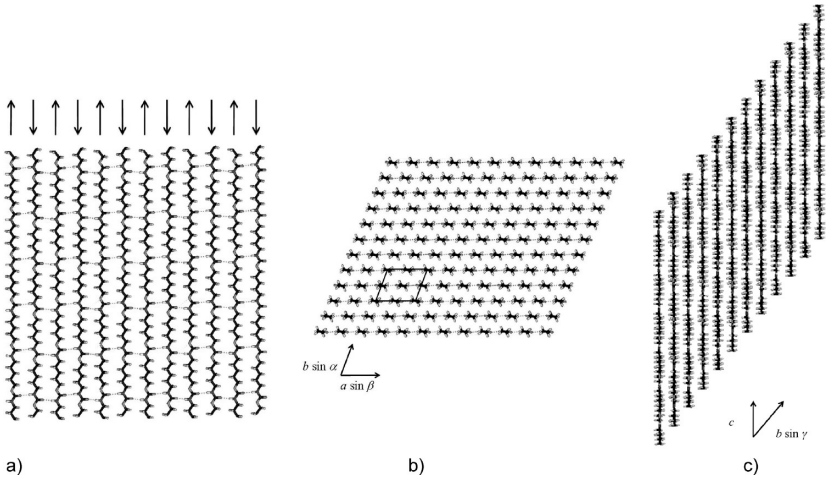

Figure 9. Schematic representation of the crystal lattice of 5-PUR. (a) Hydrogen-bonded sheet plane (*ac* plane) with hydrogen bonds set in the normal scheme. (b) Projection along the *c*-axis with hydrogen-bonded sheets displaced along the *a*-axis so that chains along the *b*-axis are in antiparallel arrangement. (c) Projection along the *a*-axis showing the shift of the chains along the *c*-axis.

distributed in the overall crystal space. The shift along the *a*-axis is such that one chain is located nearly equidistant from their six neighbors with a separating distance fluctuating between 0.4 and 0.5 nm.

Since diffraction data obtained for even *n*-PUR are essentially the same as those obtained for the odd series, a similar crystal lattice may be put forward. In this case the parameters of the triclinic unit cell matching optimally diffraction data are $a = 0.960$ nm, $c = 2(n + 3) \times 0.122$ nm and $\beta = 90°$ with α and β angles taking values around 48° and 70° respectively. Minor deviations from odd nylons in *a*, α and β parameters resulted upon adjusting the unit cell to the experimental values due to some slight differences in diffraction data. Conversely, differences concerning *b* and *c* axes are due to the presence of the 2_1 symmetry displayed by the even *n*-PUR chain. The 2-fold axis requires doubling the *c* parameter but makes unnecessary doubling the *b*-axis; since sheets are identical (they are nonpolar), a unique arrangement is feasible regarding their mutual orientation and the lattice would repeat every sheet along the *b* direction.

One striking point of this study is that X-ray diffraction of even *n*-PUR is clearly distinguished by the presence of the reflection at 0.40−0.41 nm which is absent in the odd *n*-PUR series. Such reflection is seen with medium intensity for 6-PUR and decays with *n* to vanish almost completely for 12-PUR (Figure 6b). The occurrence of a second polymorph making feasible the indexing of this reflection as *hk*0 is in disagreement with the structural behavior observed for *n*-PUR upon heating (see below).

McKiernan et al.[9,10] reported recently on the structure of *m,n*-PUR containing long polymethylene segments and attributed the presence of a reflection of similar characteristics to the scattering generated by *hkl* planes. We found indeed that the 0.40−0.41 reflection could be indexed as *hk*1, more specifically as 201/211, and noticed that it is present in the ED patterns recorded from tilted samples. The fact that this reflection decreases in intensity with *n* along the even series and becomes absent in the odd series could be due to canceling effects on structure factors.

It should be finally noticed that since two of the three unit cell axes are doubled in the two series, the unit cell contains four chains in both series. As indicated in Tables 1 and 2, the density calculated for the proposed lattices are in excellent agreement with values estimated experimentally in all cases. A schematic representation of the crystal lattice is depicted in Figure 9 using 5-PUR for illustration.

Energy Calculations and Modeling. An energy minimization analysis was carried out in order to estimate comparatively the stability of the different structures for *n*-PUR that are compatible with the experimental data obtained by diffraction analysis. Molecular mechanics energy calculations were performed by using the TINKER package, considering a modified version of the MM3 force-field. Periodic boundary conditions were applied in three directions of space, so infinite chains were considered.

Odd n-PUR: Hydrogen-Bond Scheme and Orientation of Polar Sheets. The normal and oblique hydrogen-bond schemes were compared for 5-PUR. A single infinite hydrogen-bonded sheet, with explicit inclusion of 4 dimer-chains was considered. Optimization of both structures showed that the normal scheme was energetically more favored with an energy difference of about 0.20 kcal·mol^{-1} of repeating unit. The polar forms (successive hydrogen-bonded sheets with amide dipoles pointing out to the same direction) for 5-PUR were then compared with the nonpolar forms (successive sheets alternating in polarity). The polar forms were always less favored than the nonpolar ones, with an energy surplus difference of about 2 kcal·mol^{-1} of repeating unit. Moreover, when the unit cell was allowed to relax, significant alteration of the experimentally cell parameters were observed for the polar form. The same results were obtained for both normal and oblique hydrogen-bonded sheets.

Odd- and Even n-PUR: Crystal Structure. An infinite crystal was considered for each *n*-PUR with chains in the sheets arranged in the normal hydrogen-bond scheme for both series. The periodic system consisted of a box explicitly including 4 sheets, each one with 4 dimer-chains, *i.e.*, 32 monomer repeating units, and with fixed crystal lattice parameters taken from Tables 2 and 3. Sheets were stacked with a progressive displacement along the *c*-axis direction (about 3−4 main chain atoms according to unit cell data given in Tables 2 and 3) and with alternating opposite polarity orientation in the case of the odd series. Both the *parallel* and *antiparallel* arrangements of chains along the *b*-axis were analyzed and energetically compared. As it is summarized in Table 4, the energy values obtained by minimization show that both arrangements have similar stability with energy differences being less than 0.30 and 0.40 kcal·mol^{-1} of repeating unit for the odd and even series,

respectively. These data reveal that stability differences between the two arrangements are very small so a random mixture of them most likely occurs in the real structure. Maybe worthy to point out however that, within the small range of energy values, the *antiparallel* arrangement appears to be favored in the odd *n*-PUR where the opposite seems to happen in the even series.

Energy minimization with optimization of unit cell parameters (leaving free b, α and γ parameters) was also carried out. Energy differences between *parallel* and *antiparallel* arrangements were even smaller than when unit cell parameters were fixed (around 0.10 and 0.20 kcal·mol^{-1} of repeating unit for the odd and even series, respectively). Furthermore, deviations of the parameters for the optimized structure were small, usually less than 5%. These results are given in detail in the ESM.

Table 4. Compared Energy (in kcal·mol^{-1} of Repeating Unit) for the Two Feasible Arrangements of Chains along the *b*-Axis

n-PUR	arrangement	ΔE	*n*-PUR	arrangement	ΔE
5-PUR	parallel	0.04	6-PUR	parallel	0.00
	antiparallel	0.00		antiparallel	0.04
7-PUR	parallel	0.24	8-PUR	parallel	0.00
	antiparallel	0.00		antiparallel	0.32
9-PUR	parallel	0.00	10-PUR	parallel	0.00
	antiparallel	0.01		antiparallel	0.38
11-PUR	parallel	0.19	12-PUR	parallel	0.00
	antiparallel	0.00		antiparallel	0.20

Heating Effects on the *n*-PUR Crystal Structure. The melting behavior of *n*-PUR has been examined recently and their crystallization kinetics established using the Avrami approach.[13] *n*-PUR display sharp melting at temperatures within the 119−170 °C range (Table 1) and all are able to crystallize from the melt with a good reproducibility in both melting temperature and enthalpy. Now we have investigated the structural changes that take place in the crystalline phase as well as the alterations undergone by the hydrogen bonds upon heating and cooling in a range of temperatures going from room to above melting by using real time X-ray diffraction and infrared spectroscopy.

It is widely known that polyamides usually show the Brill transition upon heating at temperatures close to melting. This transition is described as a crystalline transformation from a triclinic to pseudohexagonal phase and it is revealed by the fact that the 100/110 reflection related to the intrasheet/interchain distance and the 010 reflection related to the intersheet distance merge into a single reflection. The true nature of the Brill transition regarding hydrogen bonding is still controversial; the predominant interpretation assumes that the hydrogen-bonded structure is maintained throughout the transition.[25] The Brill transition is strongly dependent on molecular structure and crystallization conditions. At difference with nylons, no study exploring the occurrence of this transition in polyurethanes has been reported.

With the aim of knowing the effect of temperature on the crystal structure of *n*-PUR, a systematic analysis of the changes taking place in the diffraction pattern produced by

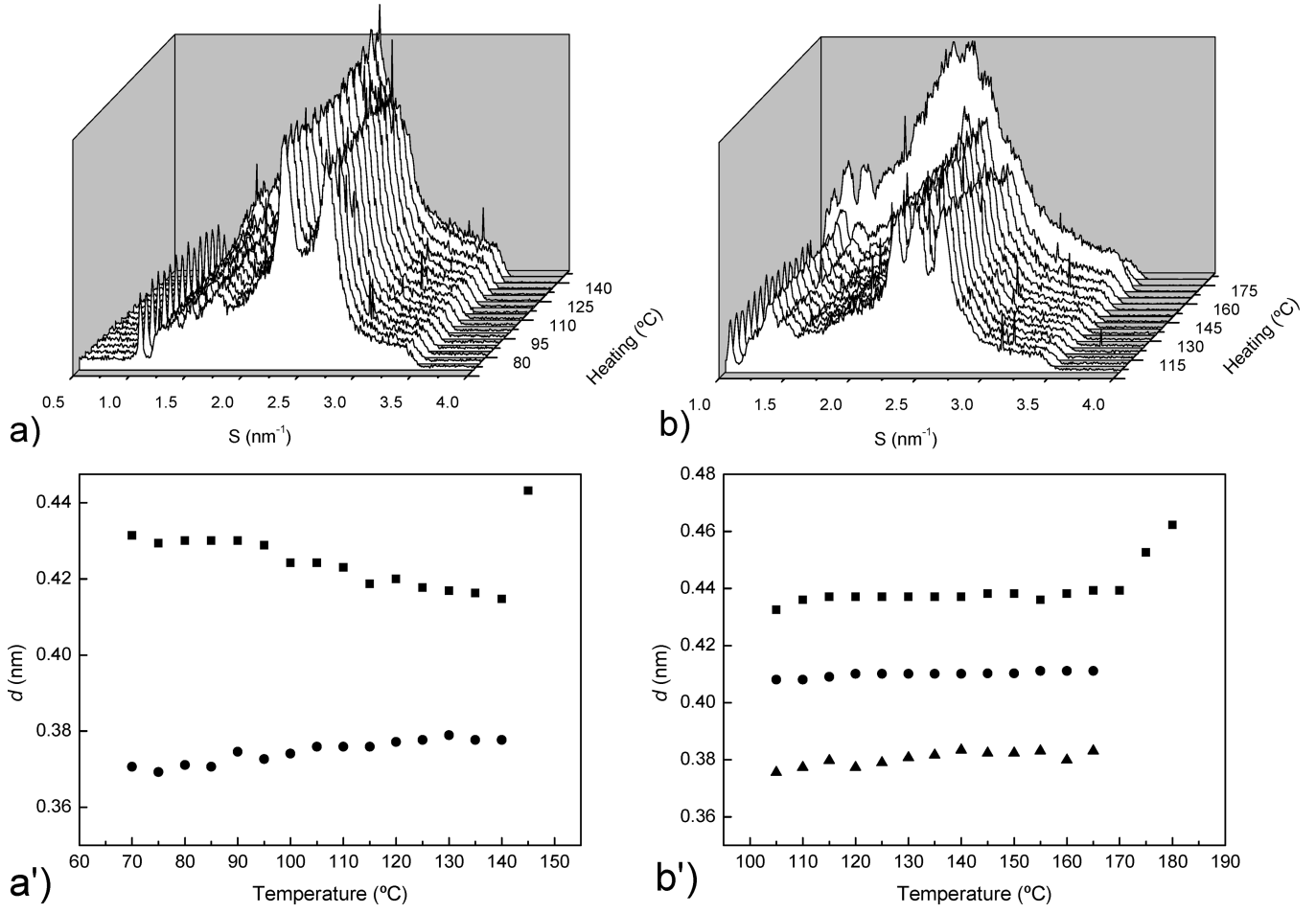

Figure 10. (a and b) Real time X-ray diffraction profiles recorded from 5-PUR and 6-PUR at heating from room temperature up to 210 °C. (a′ and b′) Evolution of the 200 and 020/220 spacings (5-PUR), and 200, 010/210 and 201/211 spacings (6-PUR) with temperature.

Table 5. Heating Effects on the Structure of *n*-PUR

	WAXS ($d_{h00}/d_{0k0/hk0}$)[a]		FTIR ($A_O/A_D/A_F$)[b]		
n-PUR	I	II	I	II	III
5-PUR	1.16	1.09	65/25/10	20/35/45	0/60/40
7-PUR	1.17	1.11			
9-PUR	1.18	1.08			
11-PUR	1.19	1.14			
6-PUR	1.15	1.15	60/25/15	30/30/40	0/50/50
8-PUR	1.15	1.14	55/25/20	30/35/35	0/40/60
10-PUR	1.14	1.13	50/30/20	35/25/40	0/45/55
12-PUR	1.14	1.13	50/40/10	20/40/40	0/55/45

[a] Spacing ratio determined by WAXS; I: room temperature and II: just before melting. [b] Ratio of ordered (A_o), nonordered (A_D) and free (A_F) CO: I, at room temperature; II, at melting; III, at 30 °C above melting.

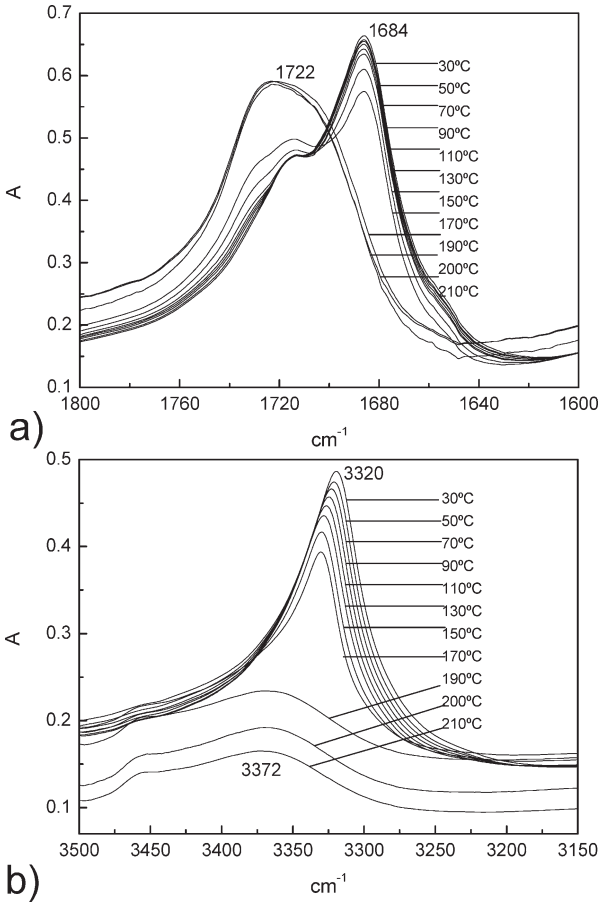

Figure 11. IR spectral changes observed for 6-PUR upon heating from room temperature up to 210 °C: (a) CO region; (b) NH region.

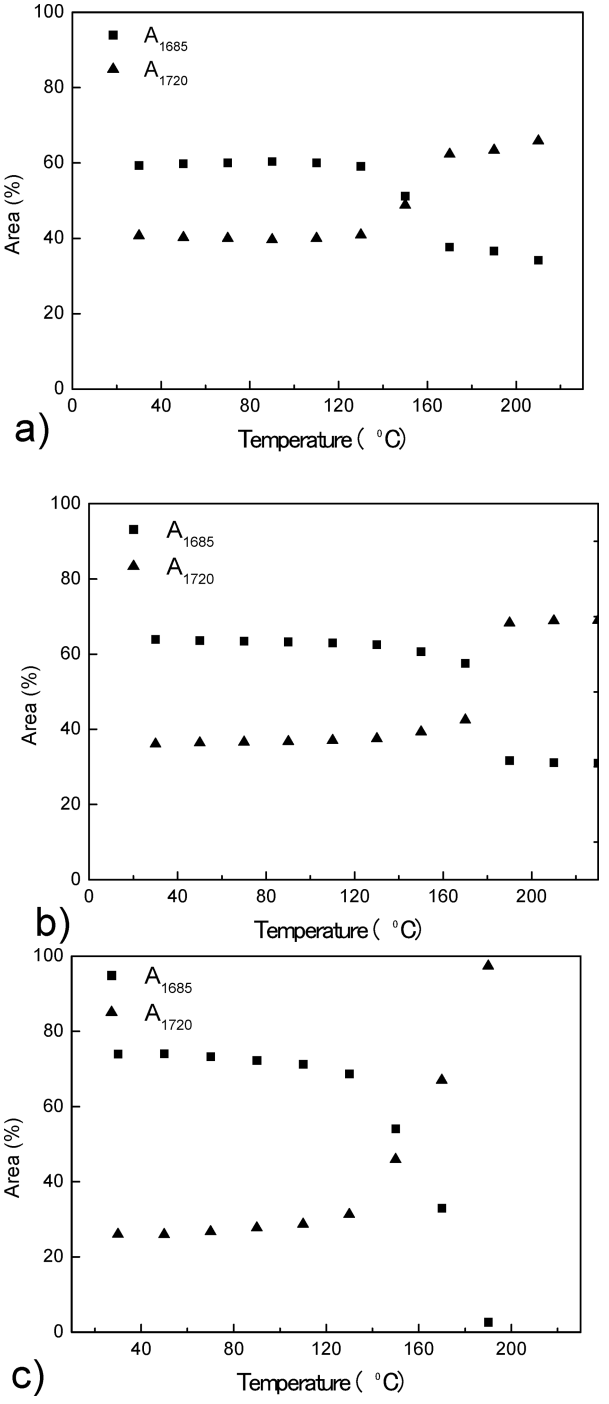

Figure 12. Evolution of the % of 1685 and 1720 cm^{-1} band areas with temperature for 5-PUR (a), 6-PUR (b), and 12-PUR (c).

these polymers has been carried out for the whole family. The wide-angle powder X-ray diffraction profile was recorded with synchrotron light from samples subjected to heating at a rate of 10 °C·min^{-1}. The results obtained for 5-PUR and 6-PUR are shown in Figure 10. A slight continuous decreasing and increasing is simultaneously observed for the *h*00 and 0*h*0/*hk*0 reflections respectively for the case of 5-PUR whereas almost no variation occurred in the scattering of 6-PUR. The illustrated behavior is representative for their respective series and results obtained for each *n*-PUR are compared in Table 5. It seems that odd *n*-PUR behave similarly to nylons with the two spacing seen at room temperature converging toward just one of intermediate value upon heating. However occurrence of melting prevents the Brill transition to be completed, which otherwise would take place at temperatures between 200 and 240 °C. On the contrary, the crystal structure of even *n*-PUR appeared to be more stable without showing any clear trend to convergence. The Brill transition entails the sliding of neighboring sheets and the fact that this movement is forbidden in the even series but not in the odd series has to be imputed to differences in the hydrogen-bonded sheet interactions existing between them.

To determine when and how much hydrogen bonding occurred during melting and crystallization, the NH and CO stretching absorption regions of 5-PUR and even *n*-PUR were examined using variable temperature FTIR spectroscopy. The infrared absorption displayed by NH and CO groups in polyamides and polyurethanes are associated with

a distribution of distances and geometries of hydrogen bonds.[9,26−28] Coleman et al. reported that hydrogen-bonded CO groups with a well-ordered geometry, such as it happens to occur in the crystalline state, show the stretching absorption band around 1685 cm^{-1}. On the other side, the free CO as it is found in the liquid nonassociated state will absorb at 1732 cm^{-1}. Hydrogen-bonded CO groups with intermediate structures, *i.e*. nonordered structures, give absorption bands around 1705 cm^{-1}. For illustration the NH and CO stretching regions of the IR spectra of 6-PUR registered at heating within the temperature range of 30−210 °C are shown in Figure 11. Upon heating, the initial 1685 cm^{-1} CO absorption band remained essentially unchanged until the temperature arrived to 150 °C where it split, generating a second broad peak centered around 1720 cm^{-1} which did not become unique up to above 190 °C. A similar behavior was observed in the NH stretching region with the 3320 cm^{-1} band observed for crystallized *n*-PUR disappearing above 150 °C at expenses of the growing of a new peak at 3370 cm^{-1}. The process was proven to be fully reversible and observed for other studied *n*-PUR, both even and odd, taking place with similar characteristics and at transition temperatures increasing correlatively with the corresponding melting temperatures (data available in the ESM file). The relative areas of bands at 1685 and 1720 cm^{-1} were estimated by deconvolution and their percentage plotted against temperature in Figure 12 to show the advance in hydrogen bonding disruption upon heating. It should be noticed that these bands are complex since both include a portion of disordered associated CO, in the first one besides the well-ordered CO present in the crystal phase, and in the second one besides the fully free CO. The conclusion drawn from this analysis is that well-ordered hydrogen bonds do not start to decompose up to the proximities of melting and that the amount remaining just after melting is about 20−30% to disappear completely at temperatures of about 30 °C above. The NH stretching region in the spectra of some *n*-PUR displayed the presence of a second shoulder at the proximities of 3450 cm^{-1} which should correspond to fully free NH. Deconvolution of the 1685 and 1720 cm^{-1} bands in their components (1685, 1705, and 1732 cm^{-1}) in an attempt of approaching to a quantitative estimation of the amount of free CO present at high temperature revealed that its content is roughly 50% of the total, the other left being associated in the disordered state (Table 5). The infrared changes observed along this study have much in common with those previously reported for semicrystalline polyamides.[26,27] Furthermore, pioneering studies carried out with *m,n*-PUR have shown that the amount of free CO groups in 6,4-PUR (a polyurethane with a density of urethane groups close to 5-PUR and a T_m = 182 °C) at 200 °C is around 40%.[28] Recent studies on new *m,n*-PUR containing long alkylene segments reported that the melt consisted of highly interacting chains with more than 75% of CO groups still hydrogen-bonded. It can be concluded therefore that the response of *n*-PUR to heating regarding hydrogen bonding is similar to that displayed by *m,n*-PUR. Since the polyurethanes retain a predominant amount of hydrogen bonds after melting, the melting enthalpy must be used mainly to break up the crystalline alkane segments contained in the polymer.

Conclusions

Aliphatic linear *n*-PUR containing polymethylene segments of length between 5 and 12 units have been isothermally crystallized in dilute solutions to render lamellar crystals with a thickness between 5 and 9 nm. Electron and X-ray diffraction data recorded from these lamellae and from powdered samples were used to analyze their crystal structure. It was found that these polyurethanes crystallized in a layered triclinic lattice with chains in fully extended conformation forming hydrogen-bonded sheets that stack progressively along the *c*-axis (chain axis) of the structure. Energy calculations gave support to the odd *n*-PUR model with hydrogen bonds set between *antiparallel* chains and sheets stacking along the *b*-axis with alternating polar orientation. The conclusion is that the crystal structure of *n*-PUR is very similar to that of *n*-nylons in both the odd and the even series with small differences due to the different symmetry displayed by the polymer chain in each case. The variable temperature analysis revealed that, as in nylons, a good amount of *n*-PUR remained associated by hydrogen bonding after melting. On the contrary, they did not show the Brill transition evidencing the higher resistance to sliding that polyurethane chains have respect to analogous polyamide chains.

Acknowledgment. Financial support for this work was provided by CICYT (Spain) with grant MAT2006-13209-C02-02. Authors are indebted to AGAUR for the Ph.D. grant awarded to Carlos E. Fernández. The Dutch work was financially supported by the Council of Chemical Sciences of The Netherlands Organization of Scientific Research (NWO−CW). Facilities provided by European synchrotron installations ESRF (Grenoble, France) and DESY (Hamburg, Germany) are acknowledged

Supporting Information Available: Text giving experimental details, figures showing TEM micrographs of lamellar crystals, evolution of the X-ray diffraction profiles, FTIR spectra, and calculations for unit cell parameter determination, and tables of energy optimization data. This material is available free of charge via the Internet at http://pubs.acs.org.

References and Notes

(1) Wirspza, Z. *Polyurethanes: Chemistry, Technology and Applications*: Ellis Horwood: London, 1993.
(2) Krol, P. *Prog. Mater. Sci.* **2007**, *52*, 915.
(3) Bayer, O. *Angew. Chem.* **1947**, *59*, 257.
(4) Versteegen, R. M.; Sijbesma, R. P.; Meijer, E. W. *Angew. Chem., Int. Ed.* **1999**, *38*, 2917.
(5) Neffgen, S.; Kusan, J.; Fey, T.; Keul, H.; Höcker, H. *Macromol. Chem. Phys.* **2000**, *201*, 2108.
(6) Kusan, J.; Keul, H.; Höcker, H. *Macromol. Symp.* **2001**, *165*, 63.
(7) Saito, Y.; Nansai, S.; Kinoshita, S. *Polym. J.* **1972**, *3*, 113.
(8) Saito, Y.; Hara, K.; Kinoshita, S. *Polym. J.* **1982**, *14*, 19.
(9) McKiernan, R. L.; Heintz, A. M.; Hsu, S. L.; Atkins, E. D. T.; Penelle, J.; Gido, S. P. *Macromolecules* **2002**, *35*, 6970.
(10) McKiernan, R. L.; Sikorski, P.; Atkins, E. D. T.; Gido, S. P.; Penelle, J. *Macromolecules* **2002**, *35*, 8433.
(11) McKiernan, R. L.; Gido, S. P.; Penelle, J. *Polymer* **2002**, *43*, 3007.
(12) Lebedev, B.; Kulagina, T.; Smirnova, N.; Markin, A.; Meijer, B.; Versteegen, R. *Macromol. Chem. Phys.* **2004**, *205*, 230.
(13) Fernández, C.; Bermúdez, M.; Versteegen, R. M.; Meijer, E. W.; Muller, A. J.; Muñoz-Guerra, S. *J.Polym. Sci. Part B Polym. Phys.* **2009**, *47*, 1368.
(14) Aharoni, S. M. *n-Nylons: Their Synthesis Structures and Properties*; Wiley: Chichester, U.K., 1997.
(15) Holmes, D. R.; Bunn, C. W.; Smith, D. J. *J. Polym. Sci.* **1955**, *17*, 159.
(16) Kinoshita, Y. *Makromol. Chem.* **1959**, *33*, 1.
(17) Slichter, W. P. *J. Polym. Sci.* **1959**, *36*, 259.
(18) Vogelson, D. C. *J. Polym. Sci., Part A* **1963**, *1*, 1055.
(19) Prieto, A.; Montserrat, J. M.; Muñoz-Guerra, S. *J. Mater. Sci.* **1990**, *25*, 2091.
(20) Muñoz-Guerra, S.; Prieto, A.; Montserrat, J. M.; Sekiguchi, H. *J. Mater .Sci.* **1992**, *27*, 89.
(21) Bermúdez, M.; León, S.; Alemán, C.; Muñoz-Guerra, S. *J. Polym. Sci., Part B* **2000**, *38*, 41.

(22) Bermúdez, M.; León, S.; Alemán, C.; Muñoz-Guerra, S. *Polymer* **2000**, *41*, 8961.
(23) Bunn, C. W.; Garner, E. V. *Proc. R. Soc. London* **1947**, *A189*, 39.
(24) Atkins., E. D. T.; Hill, M. J.; Veluraja, K. *Polymer* **1995**, *36*, 35.
(25) Brill, R. *J. Prakt. Chem.* **1942**, *161*, 49.
(26) Skrovanek, D. J.; Howe, S. E.; Painter, P. C.; Coleman, M. M. *Macromolecules* **1985**, *18*, 1676.
(27) Skrovanek, D. J.; Painter, P. C.; Coleman, M. M. *Macromolecules* **1986**, *19*, 699.
(28) Coleman, M. M.; Lee, K. H.; Skrovanek, D. J.; Painter, P. C. *Macromolecules* **1986**, *19*, 2149.